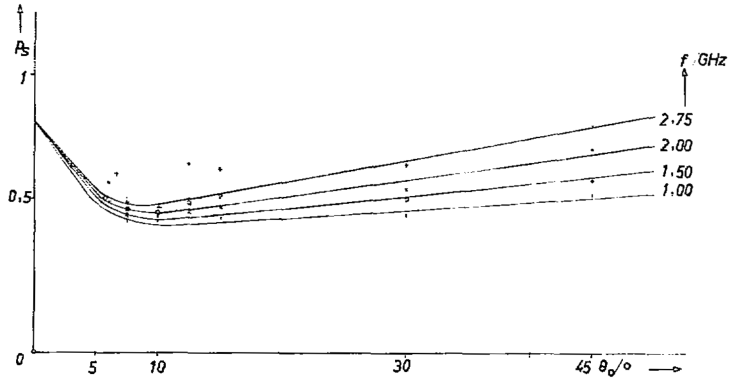

Fig. 1. Relative phase velocity along spiral arm $p_s = g$ (half-opening angle of cone θ_0). Pitch angle of spiral line $\alpha = 80$ degrees. |—1 GHz; ○—1.5 GHz; ×—2 GHz; +—2.75GHz.

tions, depending strongly on the phase velocity p, relative to the free-space velocity c_0, lead to unsatisfactory pattern forms. Because of the conical form of this antenna, the method of phase measurement in the near field using simple shorting rings, proposed by Wu [3], could not be applied here. So we used the technique with a probe whose backscattered signal was modulated by light [4], [5]. The antenna models on which the measurements were performed [6] consisted of a cone of 3.0 cm upper truncation diameter, 20 cm height, and with 2.5 cells of arm length [7]. The half-opening angle of the cone varied between 3 and 45 degrees, corresponding to the spherical coordinate system [1], as shown in Fig. 1. The operating frequency varied between 1 and 2.75 GHz. The relative phase velocity on the spiral arm is p_s. In Fig. 1 the slow-wave character of this foil-type antenna is shown very well; p_s remains lower than 0.76 in the interval named above. In the region 4 degrees $<\theta_0<15$ degrees, p_s is rather constant (smaller frequency dependence), a fact which has been stated elsewhere [8].

The far-field forms of E_θ and E_Φ, calculated by using the p_s values shown in Fig. 1, gave more efficient results [9] than those in [1]. If θ_0 increases more (>15 degrees), the p_s curves have greater divergence. In the lower θ_0 region (<4 degrees) the measurement gave rather deviating values, however, and a helical-like behavior can be expected, which was investigated on a dielectric loaded helix by Chu and Kilcoyne [10].

The equation of the curves of Fig. 1 can be approximated to an accuracy of 4 percent by the following equation:

$$p_s = 0.327 \exp(-a\cdot\theta_0) + b\cdot\theta_0 + p_s'$$

where $a = 0.31$, $p_s' = 0.42$, and b depends on the frequency as shown in the following table:

f/GHz	1.00	1.50	2.00	2.75
b	0.001 68	0.003 12	0.004 6	0.006 9

In any case it must be noted that the statement $p_s \approx 1$, given by McClelland [11] for a tube-type logarithmic spiral antenna, cannot be transferred to the foil type which is self-complementary in design [12].

III. Conclusion

It appears more effective to achieve size reduction of the antenna [13] to half of its length by choosing a loading material with $n = \sqrt{\epsilon_r \cdot \mu_r} \approx 12$, which corresponds to the p_{sz}, the phase velocity (relative) 0.07 in the z direction of the antenna, the rotation axis of the cone.

Acknowledgment

The authors wish to thank Prof. Dr. H. Lueg for helpful discussions.

Rüdiger Anders
Rolf Wohlleben
Inst. f. Tech. Elektronik
Aachen, Germany

References

[1] W. T. Cathey, "A study of the logarithmic spiral antenna wound on a cone of elliptical cross section," Ph.D. dissertation, Yale University, New Haven, Conn., 1963.

[2] B. R. S. Cheo, V. H. Rumsey, and W. J. Welch, "A solution to the frequency-independent antenna problem," *IRE Trans. Antennas and Propagation*, vol. AP-9, pp. 527–534, November 1961.

[3] P. R. Wu, "On the measurement of a bifilar complementary helical antenna," *IEEE Trans. Antennas and Propagation (Communications)*, vol. AP-15, pp. 700–701, September 1967.

[4] R. Anders and R. Wohlleben, "Ein einfaches Meßsystem nach dem Rückstreuverfahren zur Untersuchung des Antennennahfeldes nach Betrag, Phase und Richtung," *Proc. URSI-NTG-Tagung Antennen und elektromagnetische Felder* (Darmstadt, Germany, 1967). Frankfurt, Germany: VDE-Verlag, 1968, pp. 35–37.

[5] R. Anders, "Ein einfaches Meßsystem nach dem Rückstreuverfahren zur Untersuchung des Antennennahfeldes nach Betrag, Phase und Richtung," *NTZ*, pp. 271–278, May 1968.

[6] U. Engelbrecht, "Phasenbelagsmessungen an zweiarmigen, kegelförmigen, logarithmischen Spiralantennen," Technische Hochschule, Aachen, Germany, WA 221, ITE, pp. 7–98, 1967.

[7] R. Wohlleben and B. Schumacher, "Randlinienabwicklung der zweiarmigen, selbstkomplementären konischen, logarithmischen Spiralantenne," *NTZ*, pp. 585–590, October 1966.

[8] J. D. Dyson, "The characteristics and design of the conical log-spiral antenna," *IEEE Trans. Antennas and Propagation*, vol. AP-13, pp. 488–499, July 1965.

[9] R. Wohlleben, "Strahlungszonen- und Phasenzentrum der zweiarmigen, kegelförmigen, logarithmischen Spiralantenne," Dr.-Ing. dissertation, Technische Hochschule, Aachen, Germany, Fakultät f. Elektrotechnik, July 1968.

[10] T. S. Chu and N. R. Kilcoyne, "The excitation of a dielectric-rod antenna by a helix," *IEEE Trans. Antennas and Propagation (Communications)*, vol. AP-9, pp. 416–417, July 1961.

[11] O. L. McClelland, "An investigation of the near-fields on the conical equiangular spiral antenna," M.S.E.E. thesis, University of Illinois, Urbana, 1962.

[12] H. Sahler, E. Zocher, and R. Wohlleben, "Antennen für elliptische Polarisation und ihre Meßtechnik," Forschungsberichte d. Landes Nordrhein-Westfalen, no. 1873. Cologne, Germany: Westdeutscher Verlag, 1968, pp. 101–152.

[13] S. Hong and G. Rassweiler, "Size reduction of a conical log-spiral antenna by loading with magneto-dielectric material," *IEEE Trans. Antennas and Propagation (Communications)*, vol. AP-14, pp. 650–651, September 1966.

The Admittance of Infinite Cylindrical Antennas

Some time ago the author developed a technique for the accurate theoretical determination of the admittance of cylindrical antennas driven from a coaxial line [1]. An important parameter in this theory (and in its subsequent application to finite length dipole antennas [2]) is the admittance of an infinite antenna Y_f when the source of the fields is taken to be a frill of magnetic current

$$L\theta(r) = \begin{cases} -\dfrac{2V}{r\ln(b/a)}, & a < r < b,\ z = 0 \\ 0, & r > b,\ z = 0. \end{cases}$$

Table I
Admittance of Infinite Antennas*

	b/a				
ka	1.2	1.6	2.0	3.0	4.0
0.02	4.51 + i 3.88	4.51 + i 2.35	4.51 + i 2.25	4.51 + i 2.09	4.51 + i 1.96
0.04	5.44 + i 4.85	5.44 + i 3.34	5.44 + i 3.10	5.44 + i 2.81	5.44 + i 2.55
0.06	6.17 + i 5.70	6.17 + i 4.12	6.17 + i 3.78	6.16 + i 3.27	6.15 + i 2.95
0.08	6.80 + i 6.72	6.79 + i 4.83	6.79 + i 4.35	6.78 + i 3.75	6.77 + i 3.23
0.10	7.36 + i 7.44	7.36 + i 5.42	7.36 + i 4.85	7.34 + i 4.00	7.31 + i 3.45
0.12	7.89 + i 8.24	7.89 + i 5.98	7.88 + i 5.28	7.85 + i 4.26	7.81 + i 3.60
0.14	8.39 + i 8.93	8.39 + i 6.61	8.38 + i 5.69	8.34 + i 4.49	8.27 + i 3.70
0.16	8.87 + i 9.56	8.86 + i 7.01	8.85 + i 6.04	8.79 + i 4.67	8.69 + i 3.77
0.18	9.33 + i 1.02	9.32 + i 7.42	9.30 + i 6.37	9.22 + i 4.83	9.09 + i 3.81
0.20	9.78 + i 2.47	9.76 + i 7.84	9.74 + i 6.68	9.64 + i 4.94	9.46 + i3.80

* Y_f in millimhos.

Manuscript received September 26, 1968. This work was supported in part by Contract NAS 5-11543 between NASA and the Ohio State University Research Foundation.

The resultant equation for Y_f was shown to be

$$Y_f = \frac{2i\pi}{Z_0\{\ln(b/a)\}^2} \cdot \int_0^\infty \frac{\{J_0(vka)Y_0(vkb) - J_0(vkb)Y_0(vka)\}^2\, dv}{v\sqrt{v^2-1}\,\{J_0^2(vka) + Y_0^2(vka)\}}.$$

However, no numerical results were published. Therefore, in Table I some values of Y_f as a function of ka, b/a are given. The numerical integration procedure is straightforward and has been discussed adequately in the literature [3].

D. V. Otto[1]
ElectroScience Lab.
Dept. of Elec. Engrg.
Ohio State University
Columbus, Ohio 43212

References

[1] D. V. Otto, "The admittance of cylindrical antennas driven from a coaxial line," *Radio Sci.*, vol. 2, no. 9, pp. 1031–1042, 1967.
[2] ——, "Fourier transform method in cylindrical antenna theory," *Radio Sci.*, vol. 3, no. 11, 1968.
[3] E. Hallen, *Electromagnetic Theory.* New York: Wiley, 1962.

---

[1] On leave from the University of Auckland, Auckland, New Zealand.

Electromagnetic and Optical Behavior of Two Classes of Dielectric Lenses

Abstract—**Two families of spherically symmetric dielectric lenses are considered. Their optical properties are studied, and the radial eigenfunctions describing the electromagnetic field inside the lenses are found in terms of hypergeometric functions. Among the members of these two families are the Luneburg lens, the Maxwell fisheye, the isotropic lens of Eaton, and a lens that behaves like a metal reflector.**

In the following we consider two families of dielectric lenses with spherical symmetry in which the refractive index $N(x) = \sqrt{\epsilon(x)}$ is a continuous function of the normalized radial distance $x = r/a$ from the center of the lens and matches the free-space value of unity at the rim $r = a$ of the lens, i.e., $N(1) = 1$. From the optical point of view a ray enters the lens at P_1 with an angle of incidence α; it is smoothly deviated along the path P_1P_2 and leaves the lens at P_2 (see Fig. 1). We indicate by R the optical length of the path P_1P_2 (normalized to the radius a of the rim), by θ the angular extension of the path as seen from the center $r = 0$, and by δ the deviation of the ray at P_2 from the direction of incidence. From the electromagnetic viewpoint the field inside the lens can be expressed as a sum of TE and TM modes by a well-known extension of the vector wavefunction method of Hansen and Stratton (see, for example, [1]). Thus the problem is reduced to the solution of the two differential equations

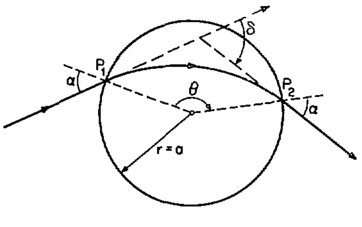

Fig. 1. Geometry for the optical ray path.

$$\frac{d^2S_n}{dx^2} + \left[\lambda^2\epsilon(x) - \frac{n(n+1)}{x^2}\right]S_n = 0 \quad (1)$$

$$\frac{d^2T_n}{dx^2} - \frac{\epsilon'(x)}{\epsilon(x)}\frac{dT_n}{dx} + \left[\lambda^2\epsilon(x) - \frac{n(n+1)}{x^2}\right]T_n = 0 \quad (2)$$

where $\lambda = ka$, k is the free-space wavenumber, n is a positive integer, and S_n and T_n are the radial eigenfunctions corresponding respectively to the TE and TM modes. For dielectric lenses we need those solutions $S_n^{(1)}$ and $T_n^{(1)}$ of (1) and (2) which are finite over $0 \leq x \leq 1$. For this reason the exact solutions of (1) and (2) are usually needed even if high-frequency estimates of the field are desired because direct asymptotic expansions of S_n and T_n, such as the WKB solutions, are usually not uniformly valid over the entire interval $0 \leq x \leq 1$.

The first class of lenses is described by the refractive index

$$N(x) = x^{1/b-1}(2 - x^{2/b})^{1/2} \quad (3)$$

where b is any positive real constant. It embodies the Luneburg lens ($b = 1$) and the isotropic Eaton lens ($b = 2$). All these lenses have the following optical properties:

$$R = b\left(\frac{\pi}{2} + \cos\alpha\right)$$
$$\theta = b(\pi - \alpha) \quad (4)$$
$$\delta = \pi(b-1) + \alpha(2-b).$$

The solution $S_n^{(1)}$ of (1) with $\epsilon = N^2$ given by (3) which is finite in $0 \leq x \leq 1$ is

$$S_n^{(1)}(x) = x^{n+1}\exp\left(-\frac{b}{2}\lambda x^{2/b}\right) \cdot {}_1F_1\left(\frac{1}{2} + \frac{b}{2}\left(n + \frac{1}{2} - \lambda\right); 1 + b\left(n + \frac{1}{2}\right); b\lambda x^{2/b}\right) \quad (5)$$

where ${}_1F_1$ is the confluent hypergeometric function. In the particular case $b = 1$ solution (5) coincides with the result of Tai [1]. The corresponding solution $T_n^{(1)}$ of (2) cannot be expressed in terms of well-known functions. With the substitution $y = x^{2/b}$, (2) becomes

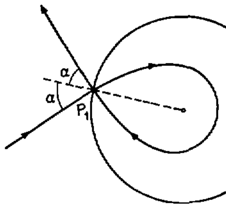

Fig. 2. The lens, $c = 2$.

$$\frac{d^2T_n}{dy^2} + \left(\frac{b}{2y} + \frac{1}{2-y}\right)\frac{dT_n}{dy} + \frac{b^2}{4}\left[\lambda^2\left(\frac{2}{y} - 1\right) - \frac{n(n+1)}{y^2}\right]T_n = 0. \quad (6)$$

This can, in turn, be reduced to the differential equation for generalized hypergeometric functions, which can be solved by power series expansions as done by Tai [1] for the particular case $b = 1$.

The second class of lenses is defined by

$$N(x) = \frac{2x^{1/c-1}}{1 + x^{2/c}} \quad (7)$$

where c is any positive real constant. It embodies the Maxwell fisheye ($c = 1$). The lenses of this family have the following optical properties:

$$R = \pi c$$
$$\theta = \pi c \quad (8)$$
$$\delta = \pi(c-1) + 2\alpha.$$

The lens corresponding to $c = 2$ presents an interesting feature: any optical ray entering the lens at P_1 bends around the center of the lens and exits at P_1 after an optical path $R = 2\pi$ which is independent of the direction α of incidence (see Fig. 2). Thus in the ideal optical limit (lossless dielectric and $\lambda \to \infty$) and aside from an irrelevant phase shift, the lens $c = 2$ behaves like a metal sphere of radius a.

The solutions $S_n^{(1)}$ of (1) and $T_n^{(1)}$ of (2) with $\epsilon = N^2$ given by (7) which are finite in $0 \leq x \leq 1$ are

$$S_n^{(1)}(x) = x^{n+1}(1 + x^{2/c})^{\beta} \cdot {}_2F_1\left(\beta + c\left(n + \frac{1}{2}\right), \beta; 1 + c\left(n + \frac{1}{2}\right); -x^{2/c}\right) \quad (9)$$

$$T_n^{(1)}(x) = x^{(2/c)\gamma_- + 1/c - 1/2}(1 + x^{2/c})^{\beta-1} \cdot {}_2F_1(\beta + \gamma_- + \gamma_+, \beta + \gamma_- - \gamma_+; 1 + 2\gamma_-; -x^{2/c}) \quad (10)$$

where

$$\beta = \frac{1}{2} - \frac{1}{2}\sqrt{1 + 4\lambda^2c^2} \quad (11)$$

$$\gamma_{\pm} = \frac{1}{2}\sqrt{1 \pm c + c^2\left(n + \frac{1}{2}\right)^2} \quad (12)$$

Manuscript received September 30, 1968. This research was sponsored by the U.S. Air Force Cambridge Research Laboratories under Contract F-19628-68-C-0071.